Influence of Structural Design Variations on Economic Viability of Offshore Wind Turbines: an Interdisciplinary Analysis

Clemens Hübler[a], Jan-Hendrik Piel[b], Chris Stetter[b], Cristian G. Gebhardt[a], Michael H. Breitner[b], Raimund Rolfes[a]

[a]*Institute of Structural Analysis, Leibniz Universität Hannover, ForWind, Appelstr. 9a, D-30167 Hannover, Germany*
[b]*Information Systems Institute, Leibniz Universität Hannover, Königsworther Platz 1, D-30167 Hannover, Germany*

Abstract

Offshore wind energy is a seminal technology to achieve the goals set for renewable energy deployment. However, today's offshore wind energy projects are mostly not yet sufficiently competitive. The optimization of offshore wind turbine substructures with regard to costs and reliability is a promising approach to increase competitiveness. Today, interdisciplinary analyses considering sophisticated engineering models and their complex economic effects are not widespread. Existing approaches are deterministic. This research gap is addressed by combining an aero-elastic wind turbine model with an economic viability model for probabilistic investment analyses. The impact of different monopile designs on the stochastic cost-efficiency of an offshore wind farm is investigated. Monopiles are varied with regard to diameters and wall thicknesses creating designs with increased lifetimes but higher capital expenditures (durable designs) and vice versa (cheaper designs). For each substructure, the aero-elastic wind turbine model yields distributions for the fatigue lifetime and electricity yield and different capital expenditures, which are applied to the economic viability model. For other components, e.g. blades, constant lifetimes and costs are assumed. The results indicate that the gain of increased stochastic lifetimes exceeds the benefit of reduced initial costs, if the overall lifetime is not governed by other turbine components' lifetimes.

Keywords: Offshore wind energy, Substructure design, Economic viability, Stochastic cost-efficiency, Lifetime distribution

List of abbreviations

APV Adjusted present value
BT Bootstrap
CAPEX Capital expenditures
CDF Cumulative density function
DECEX Decommissioning expenses
DEP Depression
DLC Design load case
DSCR Dept service cover ratio
DSC Dept service capacity
EBIT Earnings before interest, and taxes
EBITDA Earnings before interest, taxes, depreciation, and amortization
EC Environmental conditions
EMCS Equally distributed Monte Carlo simulation
FCF Free cash-flow
INT Annual interest payment
KPI Key performance indicator
IRR Internal rate of return
LCOE Levelized cost of electricity
MCS Monte Carlo simulation
NREL National Renewable Energy Laboratory
NPV Net present value
NOH Net operating hours
OPEX Annual operating expenditures
OW Offshore wind
OWT Offshore wind turbine
PDC Decomissioning provisions
PDF Probability density function
TAX Taxes on EBIT
WACC Weighted average cost of capital

1. Introduction

Although offshore wind energy is a steadily growing market [1] and a promising technology to achieve the long-term goals set for renewable energy deployment, its LCOE is still high compared to other energy supply types [2, 3]. Today, OW energy is - apart from some rare and special examples - not yet competitive without financial support mechanisms [4], as compensation according to current electricity market prices does not enable a profitable and financially viable construction and operation of OW farms. Consequently, increasing the cost-efficiency of this technology is one of the major objectives of current research. As OWT substructures and foundations account for nearly 20 % of the overall OW farm CAPEX (including planning, installation, and component costs, but excluding OPEX) and represent a significant cost reduction opportunity [2, 5], their optimal design with regard to costs and reliability is a promising approach. This means that a change in paradigm for optimal designs is required. In contrast to state-of-the-art optimization approaches, not only costs need to be minimized, but the trade-off between variable lifetimes and component costs needs to be analyzed in interdisciplinary approaches to find the most cost-efficient structural design. Nevertheless, such interdisciplinary approaches, considering both the complex engineering and economic aspects of OWT structural designs, are still unusual.
On the part of engineering analyses, most optimization approaches minimize the structural weight as a cost indicator [6–9]. Muskulus and Schafhirt [10] give a comprehensive review of these optimization approaches. Even if cost models are applied instead of mass considerations, the costs are, in general, approximated by empirical formulations taking into account material, production, and installation costs [11, 12]. The effects of reduced masses or costs on the economic viability of entire projects are not evaluated, as economic aspects, like risk-adjusted discount rates, etc., are not taken into account. Furthermore, lifetimes are set to deterministic, constant values. This disables an analysis of the trade-off between lifetime and costs. A first approach to take variable lifetimes in engineering models for OWT into account is conducted by Ziegler et al. [13]. However, they focus on the trade-off between variable lifetimes and mass, and - as typical for engineering approaches - do not consider complex economic effects.
On the part of economic analyses, substructures and foundations are, in general, considered as a bundled cost input within the CAPEX of an OW farm. Furthermore, as with the engineering analyses, the operating OWT lifetime is typically treated as a deterministic, constant value commonly set to 20 years [14–16]. In addition, several economic studies conduct simple deterministic sensitivity analyses regarding the lifetime, but do not consider any dependencies of the lifetime on other model inputs [17–19]. A first approach to analyze the effects of lifetime extension measures for onshore wind turbines on the LCOE is developed by Rubert et al. [20]. They link the lifetime to model inputs, like retrofits of different components, and also conduct deterministic sensitivity analyses. However, due to the significant variability of offshore conditions, economic effects of structural design variations are different, if probabilistic approaches are applied. Nevertheless, comprehensive probabilistic economic analyses of OW farms that take into account the complex economic effects of structural designs on the trade-off between operating lifetime and the cost of OWT cannot be found.
This research gap is addressed by combining an aero-elastic OWT model with an economic viability model. The combined model can deal with probabilistic inputs based on real offshore measurements and OW investment characteristics. An overview of the combined approach is illustrated in Fig. 1. This concept enables analyzing the effects of substructure design variations on the cost-efficiency of OW farms. Therefore, it is possible to assess the trade-off between substructure lifetime - being modeled using a probability distribution - and substructure CAPEX with regard to the cost-efficiency of each design. To this end, both models are outlined in the following and are then applied to a concise OW farm case study.

2. Aero-elastic wind turbine model

2.1. Time domain model

The dynamic OWT behavior is very complex due to several reasons: nonlinearities, transient load cases, scattering environmental conditions, highly coupled subsystems, etc. Hence, aero-hydro-servo-elastic simulations in the time domain are required by the standards [21]. One software being capable of simulating

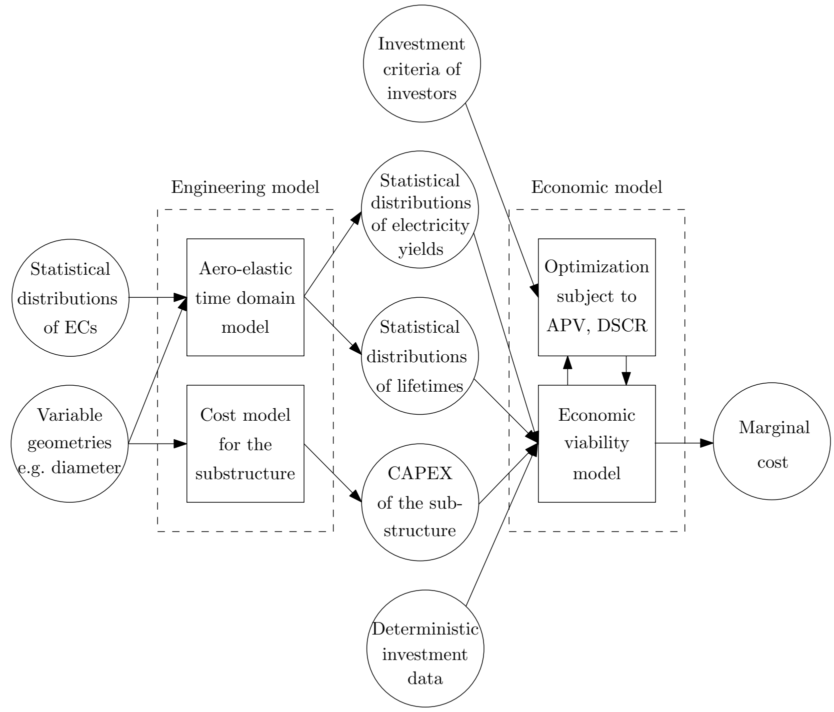

Figure 1: Visualization of the combined engineering and economic model.

these coupled systems in approximately real time and being used in this study is the FASTv8 software code by the NREL [22]. Using FAST, in this study, the NREL 5 MW reference wind turbine [23] is investigated. Well-founded reference turbines are only available for 5 MW [23] and 10 MW [24]. Since a wind farm with a commission date of 2020 - where normally 6-8 MW turbines are used - is considered (cf. Section 3.1), the use of a relatively small 5 MW turbine is justified. The corresponding OC3 phase I monopile (cf. Fig. 2) is used as substructure [25]. Slight design changes of the OC3 monopile are applied to analyze the effect of design variations on the economic viability of an entire OW farm.

Using the aero-elastic model and various EC that mirror the changing EC at the offshore site as inputs, it is possible to calculate time series of forces and moments acting on all structural components. The focus is on the design of steel substructures, so that fatigue damages are most critical. Therefore, time series are post-processed to approximate the fatigue lifetime, as described in Section 2.3. At this point, the limitation of this work to the substructure is highlighted. Constant lifetimes and costs for all other turbine parts (e.g. blades) are assumed. This approach is unproblematic as long as the substructure has a lifetime below 20 years. In this case, the lifetime of other components is not completely exploited. For substructure lifetimes above the 20-year design lifetime, this concept is questionable. A lifetime extension of other components is not always possible without significantly increasing the costs. This drawback of the present approach and some possible workarounds are discussed in Section 4.

For all simulations, the simulation length is set to 10 minutes according to current standards and previous research [21, 26]. The “run-in” time (i.e. the time that has to be removed from each time series to exclude initial transients) is set to values between 60 and 720 seconds according to Hübler et al. [26]. The turbulent wind field is calculated using the Kaimal model and the software TurbSim [27]. The JONSWAP spectrum is applied to compute irregular waves. To keep the simulation setup as simple as possible and to be in accordance with the OC3 study [25], currents, second-order and breaking waves, local vibrations, degradation effects, and soil conditions are not taken into account. These common assumptions might affect the precise lifetimes values, but do not limit the general conclusions.

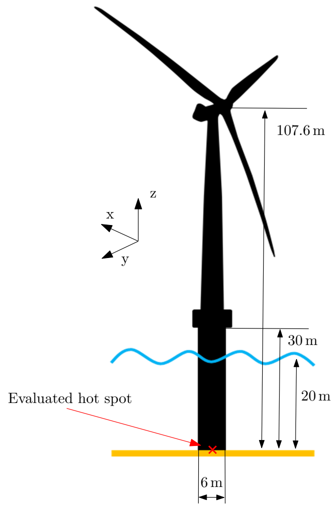

Figure 2: Visualization of the OC3 monopile and the NREL 5 MW reference wind turbine. Inertial frame coordinate system: x downwind direction, y to the left when looking downwind, and z vertically upwards.

2.2. Probabilistic simulation approach

FAST is capable of simulating time series of forces and moments for a given set of EC. Ideally, the entire (20 year) design lifetime of a wind turbine would be simulated. However, due to computational limitations, this is hardly possible. Hence, to get well-founded lifetime approximations, it is not only necessary to calculate the resulting damages of each simulation (see Section 2.3), but also to use a representative set of load cases. These load cases should mirror the entire OWT lifetime. This can either be done by applying a deterministic, DLC based approach, as proposed by current standards [21] or a probabilistic approach [28]. In any case, the damage extrapolation is based on a limited number of simulations so that fatigue damage designs become relatively uncertain. Here, a probabilistic bin based approach is utilized: the EMCS [28]. This means: The wind speed range is split up into several bins of $2\,\mathrm{m\,s^{-1}}$. In each wind speed bin, the same number of $N_{\mathrm{bin}} = 100$ simulations is conducted. The use of a relatively high number of simulations in each bin (current standards recommend at least six simulations per bin) is required, since simulation results within each bin scatter significantly. Reasons for these highly uncertain loads within one and the same bin are, first, random realizations of the turbulent wind and the sea state (i.e. random seeds) [29], and second, other statistically distributed EC (e.g. wave heights or turbulence intensities) [28]. The EC for each simulation are determined by sampling from given statistical distributions. Hence, in each bin, MCS is applied. The difference to plain MCS is that more simulations are conducted for high wind speeds having very low occurrence probabilities, but leading to relatively high damages. Therefore, depending on the damage-wind speed correlation, the intensified sampling for high wind speeds by EMCS reduces the error due to limited sampling. To illustrate the EMCS approach, Fig. 3 shows the applied sampling distribution for wind speeds, being a piecewise defined Weibull distribution and no longer the real wind speed Weibull distribution (F_{Wbl}). For a detailed description, it is referred to the original source [28].
Dependent statistical distributions for seven EC (wind speed (F_{Wbl}) and direction, turbulence intensity, wind shear and wave height, period and direction) are taken from the database in Hübler et al. [26]. For this database, measurement data of the FINO3 measurement mast in the North Sea is used.

2.3. Lifetime calculation

To approximate the substructure lifetime, the lifetime fatigue damage has to be calculated. Therefore, the forces and moments for the most critical location are needed. The applied lifetime calculation procedure

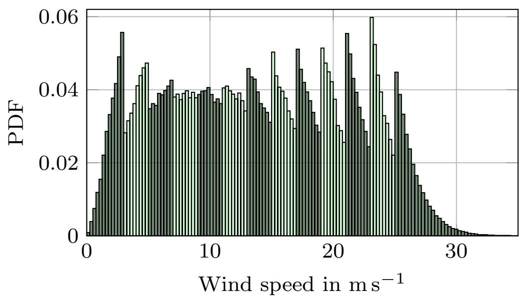

Figure 3: EMCS sampling distribution for wind speeds. Fairly homogeneous sampling due to applied bins, but in each bin samples are generated using truncated Weibull distributions and MCS leading to discontinuities at the boundaries of bins. Shading illustrates the bins.

[28] is briefly explained in the following: The monopile welds are exposed to higher fatigue damages compared to the rest of the monopile (e.g. plain steel plates), as stresses are concentrated in these hot spots (welds). Hence, in a first step, hot spot stresses are calculated according to Eurocode 3, part 1-9 [30]. As the stress concentration at transversal welds is more critical (a detail of 71 MPa according to Eurocode 3) than at longitudinal welds, only transversal welds are investigated. An additional stress concentration factor due to the size effect of the monopile wall thickness ($t > 25\,\mathrm{mm}$) is applied [30]. Since the considered monopile has a pure cylindrical shape and hot spots below mudline are not taken into account, the design driving location - being exposed to the highest bending moments - is at mudline. For this location marked in Fig. 2, the lifetime calculation is conducted.

In most cases, for monopiles, shear stresses (τ) are negligible compared to direct stresses (σ). Thence, the normal stress transverse to the weld can be approximated as follows:

$$\sigma_\perp = \frac{F_z}{A} + \frac{\sqrt{M_x^2 + M_y^2}}{S}. \tag{1}$$

Here, F and M are forces and moments (cf. Fig. 4), A is the cross section area, and S is the section modulus. This procedure is a simplification, as the maximum normal stress is assumed and a directional dependence for different load cases is neglected ($M = \sqrt{M_x^2 + M_y^2}$).

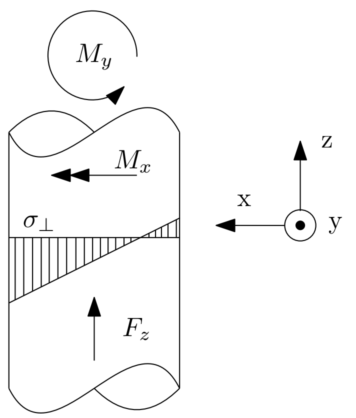

Figure 4: Illustration of relevant forces and moments acting on the monopile cross section.

For the normal stress, a rainflow counting evaluates the stress cycles and the linear damage accumulation according to the Palmgren-Miner rule is applied. The damage for each time series (j) in each wind speed bin (m) is calculated as follows:

$$D_{TS,j,m} = \sum_{i=1}^{I} \frac{n_i}{N_i}; \quad \forall j \in J(m), m \in M, \tag{2}$$

where n_i is the cycle number associated with the stress amplitude $\Delta\sigma_{\perp,i}$, N_i is the endurance (cycle number) for the same stress amplitude, and I is the number of considered stress amplitudes. M and $J(m)$ are the bin number and the number of time series depending on the bin, respectively. Since EMCS with 13 bins and 100 samples per bin is applied, it follows $M = 13$ and $J(m) = 100$. The slope of the S-N curve is set to three before and to five after the fatigue limit.

In general, the extrapolated lifetime damage (D_{LT}) is the weighted sum of the damages of all time series in all wind speed bins:

$$D_{LT} = \sum_{m=1}^{M} \sum_{j=1}^{J(m)} \left(D_{TS,j,m} \frac{J_{\text{total}} Pr(m)}{J(m)} \right), \tag{3}$$

where J_{total} is the number of total time series during the lifetime (e.g. $6 \times 24 \times 365.25 \times 20$ for a 20-year lifetime and 10-minute simulations). $Pr(m) = F_{Wbl}(b_m) - F_{Wbl}(a_m)$ is the occurrence probability of the mth wind speed bin according to the real wind speed Weibull distribution (F_{Wbl}) and decreases for high wind speeds. a_m and b_m are the minimum and maximum wind speeds of the mth bin, respectively. $Pr(m)$ is not related to the EMCS sampling distribution (piecewise defined Weibull distribution, cf. Fig. 3) that is only relevant for the sampling.

However, since yearly realizations of the EC are needed for the economic model, here, yearly damages for each year (t) are calculated first:

$$D_{year,t} = \sum_{m=1}^{M} \sum_{j=1}^{J_y(m)} \left(D_{TS,j,m} \frac{J_{\text{total,y}} Pr(m)}{J_y(m)} \right), \tag{4}$$

where $J_y(m)$ is the number of time series per year depending on the bin (assuming a lifetime of 20 years $J_y(m) = 100/20 = 5$) and $J_{\text{total,y}} = 6 \times 24 \times 365.25$ is the number of total time series during one year. Using the same EC realizations, the annual electricity yield (Y_t) is calculated:

$$Y_t = \sum_{m=1}^{M} \sum_{j=1}^{J_y(m)} \left(P(v) \frac{J_{\text{total,y}} Pr(m)}{J_y(m)} \right), \tag{5}$$

where $P(v)$ represents the realization of a cumulative power curve of all wind turbines of an OW farm at wind speed v.

The damage after T years is the sum of the yearly damages:

$$D_{sum} = \sum_{t=1}^{T} D_{year,t}. \tag{6}$$

If D_{sum} exceeds 1, the substructure lifetime (L) is reached. Hence, L can be determined by finding T^* being the last value for T where $D_{sum} < 1$. Since the end of life will normally not be reached at the end of full years, $D_{sum} = 1$ and therefore L is approximated by using partial years.

In this work, a probabilistic lifetime calculation is applied. Hence, Eqs. 4, 6, and the determination of L are not evaluated once, but $N_{BT} = 10{,}000$ times using a bootstrap algorithm. This means: Having $N_{\text{bin}} = 100$ simulation results available in each bin, 5 samples per year - corresponding to 100 samples per 20 years design lifetime - are drawn randomly with replacement from each bin. Therefore, for each bootstrap evaluation (N_{BT}), different cases ($D_{TS,j,m}$) are randomly selected which leads to varying yearly damages ($D_{year,t}$), lifetimes (L), and electricity yields (Y_t). This bootstrap approach enables an uncertainty estimation due to finite sampling in combination with varying EC and yields the lifetime PDF (cf. Fig. 5) as well as the electricity yield PDF. At this stage, it has to be clarified that the resulting variability of lifetime values is mainly due to the uncertain extrapolation process that is part of today's turbine designs. If the entire lifetime would be simulated, the variation would only be due to the long-term EC scattering, which is much smaller.

Since, for example, the reference design is not designed for the investigated OW farm site, quite damaging load cases for fault conditions are not taken into account, and safety factors - like the material safety factor - are not applied, the calculated lifetime does not match the 20-year design lifetime, but is significantly higher (by a factor of about 75). This is not problematic, since this is an exemplary study that does not intend to actually find the best design. However, to ensure reasonable results for the economic viability, substructural lifetimes have to be close to realistic project durations (typically 20 years). Therefore, all lifetimes are normalized using the 5^{th} percentile of the lifetime of the reference design (i.e. it is assumed that the reference design lifetime is at least 20 years with a probability of 95 %).

2.4. Cost model for the substructure

The cost model for the substructure CAPEX is based on Häfele and Rolfes [8]. Some changes are made to adjust this model to monopiles. For example, welding costs are significantly lower for monopiles, as the welding is automated. It is assumed that the substructure CAPEX (C_{sub}) consists of costs for the monopile (C_{mono}), the transition piece (C_{TP}), the tower (C_{tower}), and secondary components (C_{add}) (e.g. boat landings, etc.):

$$C_{sub} = C_{mono} + C_{TP} + C_{tower} + C_{add}. \tag{7}$$

Since only slight design variations are carried out, it can be assumed that transition piece, tower, and secondary components are not significantly affected. Therefore, their costs per mass can be set to constant values (see Table 1). Monopile costs are further divided into raw material costs (C_{mat}), welding costs (C_{weld}), fixed production costs (C_{prod}), and coating costs (C_{coat}):

$$C_{mono} = C_{mat} + C_{weld} + C_{prod} + C_{coat}. \tag{8}$$

Table 1: CAPEX for various parts and aspects. Adapted using several sources.

Cost type	Cost	Adapted sources
C_{TP}	2600 EUR/t	[11]
C_{tower}	2500 EUR/t	[31]
C_{add}	5900 EUR/t	[11]
C_{mat}	920 EUR/t	[11, 32]
C_{weld}	0.33 MEUR/m^3	[11, 32]
C_{prod}	0.20 MEUR	[11, 32]
C_{coat}	200 EUR/m^2	[11, 33]

Here, the material costs are proportional to the mass, the welding costs to the weld volume, and the coating costs to the surface area. For the coating costs, an initial (onshore) coating (down to 5 m below mudline) and an additional (offshore) patch coating of 2 % of the surface area are assumed. This leads to the relatively high costs per m^2.

2.5. Design of substructures

To analyze the effect of substructural design variations on lifetimes and costs, and in the end on the economic viability, a reference structure is needed. As stated in Section 2.1, this reference is the well-established OC3 monopile substructure with the NREL 5 MW turbine. In this study, seven design variations are investigated: the reference OC3 monopile, three more durable designs (with increased wall thicknesses and diameters of the monopile) and three cheaper ones (decreased thicknesses and diameters). The design changes are summarized in Table 2.

Table 2: Analyzed substructures with small design changes.

Design	Abbreviation	Change in diameter	Change in wall thickness
Reference	Ref	–	–
Design 2	D+	+1 %	–
Design 3	D−	−1 %	–
Design 4	t+	–	+2 %
Design 5	t−	–	−2 %
Design 6	Dur	+1 %	+2 %
Design 7	Chp	−1 %	−2 %

3. Economic viability model

In order to measure the cost-efficiency of substructure designs, an economic viability model for financial analyses of wind farms is applied in a simulation study of a project located in the German Exclusive Economic Zone of the North Sea. The economic viability model is an extension of the model presented in Piel et al. [34]. It simulates an economic agent to depict the investment decisions of real-world corporations investing in OW farms. The economic viability model is reformulated as an optimization problem. It yields the required minimum sales price per unit of generated electricity - the marginal cost (in ct/kWh) - for which the analyzed OW farm would exactly meet the investment criteria of both debt (see Section 3.2) and equity (see Section 3.3) investors taking into account each substructure design separately (see Section 3.4). The marginal cost is comparable to the LCOE and has a similar meaning [34]. However, as it considers the specific project finance characteristics (see Sections 3.1-3.3). It allows for more precise financial analyses of OW farms. Consequently, the marginal cost is utilized as the competitiveness criterion for the comparison of substructure designs according to the following rationale: The lower the marginal cost of the OW farm, the higher the cost-efficiency of the analyzed substructure design.

3.1. Cash-flow simulation

The economic viability model combines a state-of-the-art cash-flow calculation for OW farms oriented towards Piel et al. [34] with the MCS approach of the aero-elastic OWT model. This enables the simulation of uncertain cash-flows using the $N_{BT} = 10{,}000$ realizations provided by the aero-elastic OWT model for the annual gross electricity yield and the turbine lifetime as well as CAPEX of the different substructure designs. For every turbine of the investigated OW farm, the cash-flows are simulated until the end of the corresponding lifetime realization (i.e. no electricity is produced by a turbine after reaching its end of life, $Y_t = 0 \; \forall \; t > T^*$). The cash-flow simulation is based on an income statement and a cash-flow statement, as shown in Table 3. Both statements are simulated for each year of the project life cycle and each MCS iteration. This yields PDF estimations of the unlevered FCF, which serve as the basis for the debt sculpting in Section 3.2 and the project valuation in Section 3.3.

Table 4 shows the project characteristics of the OW farm under investigation to which the cash-flow simulation is applied. The cost data is derived from Reimers and Kaltschmitt [35] using their experience curve theory model in consideration of an estimated total installed wind energy capacity of 741.70 GW (34 GW offshore [36]) in 2020 [37]. The financing data is oriented towards the cost of capital forecast for German OW farms commissioned in 2020 from Prognos and Fichtner [5]. The tax data refers to the German tax legislation. The annual revenues $R_{i,t} = p \cdot Y_{i,t} \cdot NOH$ are calculated by multiplying the sales price per unit of generated electricity p by the gross electricity yield $Y_{i,t}$ and the net operating hours NOH in each year

Table 3: Income and cash-flow statements.

Income statement		Cash-flow statement	
	Revenues		**EBIT**
−	OPEX	−	Taxes on EBIT
=	**EBITDA**	+	Depreciation
		+	Decommissioning provision expenses
−	Depreciation	−	CAPEX
−	Decommissioning provision expenses	−	Decommissioning expenses
=	**EBIT**	=	**Unlevered free cash-flow**

Table 4: Project characteristics of the OW farm under investigation.

General data		**Cost data**	
Distance to shore	10 km	CAPEX	
Distance to port	20 km	-Project development	110 MEUR
Water depth	20 m	-Installation	2.4 MEUR/turb.
Commissioning date	01.01.2020	-Rotor, nacelle and tower	8.2 MEUR/turb.
Wind turbines	80 NREL 5 MW	-Substructure	Substructure costs
Total capacity	400 MW	-Insurance and financing	36 MEUR
OW farm efficiency	74 %	OPEX	
Net operating hours	6500 h/turb.	-Operation & maintenance	0.20 MEUR/turb.
Wind resource	Wind speed PDF	-Insurance	0.10 MEUR/turb.
Project duration	Lifetime PDF	Decommissioning expenses	0.51 MEUR/turb.
Tax data		**Financing data**	
Corporate tax	31 %	Unlevered cost of capital	5.6 %
Straight line depreciation	16 years	Cost of debt	3.5 %
Provision expenses	Discounted at 5.5 %	Debt service period	16 years

$t = (0, ..., T_i)$, where T_i represents the total project life cycle length. The net operating hours are derived from the OW farm efficiency stated in Prognos and Fichtner [5]. All probabilistic parameters are denoted by the index $i = (1, ..., N_{BT})$ with N_{BT} as the number of MCS iterations.

3.2. Debt sculpting

In recent years, OW farms were, to a large extend, funded via non-recourse project finance which typically features high shares of debt [38]. The debt-to-equity ratio can be optimized by means of a debt sculpting model based on the unlevered FCF resulting from the cash-flow simulation. Optimizing the debt-to-equity ratio utilizes the leverage effect of debt financing, which increases the profitability from equity investors' perspective, if the cost of debt is lower than the IRR [39]. In order to optimally utilize the leverage effect, the debt sculpting model yields the maximum amount of debt capital that can be raised such that the investment criteria of debt investors are exactly met. In project financing, debt investors typically consider a certain DSCR target as their investment criteria. The DSCR measures the coverage of the contractual debt service by the cash-flow available for debt service [40]. Based on the DSCR target, debt sculpting entails calculating the repayment schedule of debt capital such that the debt service, including interest payments and principal repayments, is tailored to the cash-flow available for debt service (here: unlevered FCF) [40]. Consequently, the debt sculpting ensures that a minimum DSCR is maintained in each year of the debt service period.

The DSCR is calculated as follows:

$$DSCR_{i,t} = \frac{FCF_{i,t}}{INT_t + P_t}; \quad \forall i \in N_{BT}, t \in T_{Debt}, \tag{9}$$

where $FCF_{i,t}$ is the unlevered FCF, INT_t is the annual interest payment, $P_{i,t}$ is the annual principal repayment, and T_{Debt} is the length of the entire debt service period. Based on a predefined minimum DSCR target, the maximum debt service capacity is calculated as follows:

$$DSC_t = \frac{F^{-1}_{FCF,t}(\alpha)}{\beta}; \quad \forall t \in T_{Debt}, \tag{10}$$

where $F^{-1}_{FCF,t}$ is the inverse of the unlevered FCF CDF, α is a confidence level, and β is the predefined minimum DSCR target. Both α and β represent the investment requirements of debt investors. Debt investors of OW farms are typically willing to invest, if the DSCR is equal to $\beta = 1.2$ with a confidence of $1 - \alpha = 75\,\%$ throughout all debt service periods [40]. A DSCR greater than one implies that the project is able to cover the debt service in a specific period by the FCF generated in the same period, and thus, indicates the soundness of the project corporation. Given that the debt capital is raised in form of zero coupon bonds, the maximum amount of debt capital is derived from the debt service capacity as follows:

$$D = \sum_{t=1}^{T_{Debt}} \frac{DSC_t}{(1 + r_d)^t}, \tag{11}$$

where r_d is the cost of debt. Zero coupon bonds do not pay any interest and their principal is the amount to be repaid at the time to maturity. Thus, with coupon-stripping any bond can be separated into individual securities each representing a zero coupon bond selling at different discounts depending on the time to maturity [41]. This property enables sculpting the debt to the debt service capacity in each individual debt service period such that the summed security values equal the maximum amount of debt capital to be raised. Based on the latter, the principal repayments (P_t) and interest payments (INT_t) can be calculated as follows:

$$P_t = \frac{DSC_t}{(1 + r_d)^t}; \quad \forall t \in T_{Debt} \tag{12}$$

and

$$INT_t = DSC_t - P_t; \quad \forall t \in T_{Debt}. \tag{13}$$

Due to the debt sculpting, the sum of principal repayments and interest payments is equal to the debt service capacity in each year of the debt service period. This ensures that the minimum DSCR target of the debt investors is fulfilled and the maximum amount of debt capital is raised.

3.3. Valuation

In order to enable the evaluation of the OW farm profitability, the present economic viability model utilizes the APV method to estimate a PDF of the project value by discounting the unlevered FCF to the valuation date. Following Myers [42], the APV method is applied as follows:

$$APV_i = \sum_{t=0}^{T_i} \frac{FCF_{i,t}}{(1 + r_e)^t} + \frac{\tau \cdot INT_t}{(1 + r_d)^t}; \quad \forall i \in N_{BT}, \tag{14}$$

where τ is the corporate tax rate and r_e is the unlevered cost of equity. In market-oriented financing and industrialized economies, the alternative WACC method is widely used. The APV method is applied to valuing investments in economies of high uncertainty and scarce financial markets where stable debt-to-equity ratios are hard to obtain [43]. As the latter applies to OW farms, the use of the APV method is the best choice [44]. This is due to the explicit tax-shield consideration, which represents tax advantages arising from debt financing, in the second fraction of the APV equation. The APV method enables a straightforward tax-shield adjustment for changes in the debt-to-equity ratio during the project life cycle. However, if consistently applied, the alternative WACC method with the corresponding NPV would lead to the same project value [34].

3.4. Marginal cost calculation

The combination of cash-flow simulation, debt sculpting, and APV method yields several KPI in the form of PDF. These KPI are the basis for the optimization model that quantifies the marginal cost of the analyzed OW farm. As the implementation of wind farms depends on balancing the interests of both equity and debt investors, the optimization model considers an economic agent that represents the perspectives of both groups of decision-makers. By keeping the investment behavior of real-world corporations in the realm of wind farms, the economic agent measures the soundness of the analyzed project from debt investor perspective by way of the DSCR and utilizes the APV to analyze the profitability from equity investor perspective. A simple mathematical formulation of the optimization problem is as follows:

$$\boldsymbol{Minimize}\ p \qquad \text{subject to} \tag{15}$$

$$E(APV) \geq 0 \tag{16}$$

and

$$F^{-1}_{DSCR,t}(\alpha) \geq \beta; \quad \forall t \in T_{Debt}, \tag{17}$$

where $E(APV)$ is the expected APV and $F^{-1}_{DSCR,t}$ is the inverse of the DSCR CDF. The optimization model minimizes the sales price per unit of generated electricity p by accounting for the trade-off between APV and DSCR, which is strongly influenced by the debt share. The first constraint represents the general investment requirement of the equity investors. It determines that they are willing to invest, if the expected APV is nonnegative. This is equivalent to an expected (unlevered) IRR that is equal to or greater than the (unlevered) cost of capital - a typical investment rule of equity investors of OW farms [45]. Accordingly, the second constraint represents the investment requirement of the debt investors.

In order to find an analytical solution for the optimization problem, a derivative of the expected APV with respect to p is used:

$$\frac{dE(APV)}{dp} = (1-\tau) \cdot \sum_{t=1}^{T} \frac{E(Y_t)}{(1+r_e)^t} + \tau \cdot (1-\tau) \cdot \sum_{t=1}^{T_{Debt}} \frac{\frac{F^{-1}_{Y,t}(\alpha)}{\beta}}{(1+r_d)^t} \cdot (1-(1+r_d)^{-t}), \tag{18}$$

where T is the maximum total project life cycle length for all iterations, $E(Y_t)$ is the expected electricity yield, and $F^{-1}_{Y,t}(\alpha)$ with $1-\alpha = 75\,\%$ is the 25^{th} percentile of the electricity yield. The mathematical derivation of Eq. 18 using Eq. 14 is given in Appendix A. The first addend refers to the discounting of the unlevered FCF in the APV method. The second addend refers to the discounting of the tax-shields and is based on the second constraint. By means of the revenues, the sales price per unit of generated electricity p affects the unlevered FCF as well as the tax shield. The latter is based on p due to the debt sculpting, which maximizes the amount of debt financing, and thus, determines the interest payments considered in the tax shield calculation. The derivative measures the sensitivity of changes in the expected APV with respect to a change in p.

Since the APV in Eq. 14 is linear in the price p (cf. Appendix A), the exact solution of the optimization problem can be found by means of the derivative. The cash-flow simulation, debt sculpting, and APV method are conducted using an initial guess $p_{initial} \in \mathbb{R}^+ \setminus \{0\}$. Afterwards, the minimum sales price per unit of generated electricity is calculated as follows:

$$p* = p_{initial} - \frac{E(APV)}{\frac{dE(APV)}{dp}}, \tag{19}$$

where the second subtrahend represents the change of the initial guess necessary to set the expected APV exactly to zero. As stated in Section 3, the resulting minimum sales price per unit of generated electricity $p*$ represents the marginal cost and thus the competitiveness criterion.

Table 5: Approximated substructure costs and lifetimes.

Design	Substructure costs in MEUR	Difference	Expected substructure lifetime in years	Difference	Coefficient of Variation of the lifetime
Ref	2.84	–	23.4	–	0.086
D+	2.87	+1.09 %	26.6	+13.9 %	0.091
D−	2.81	−1.09 %	22.7	−3.08 %	0.066
t+	2.88	+1.32 %	26.7	+14.2 %	0.076
t−	2.80	−1.30 %	21.0	−10.1 %	0.094
Dur	2.91	+2.46 %	30.2	+29.2 %	0.068
Chp	2.78	−2.33 %	17.3	−26.0 %	0.084

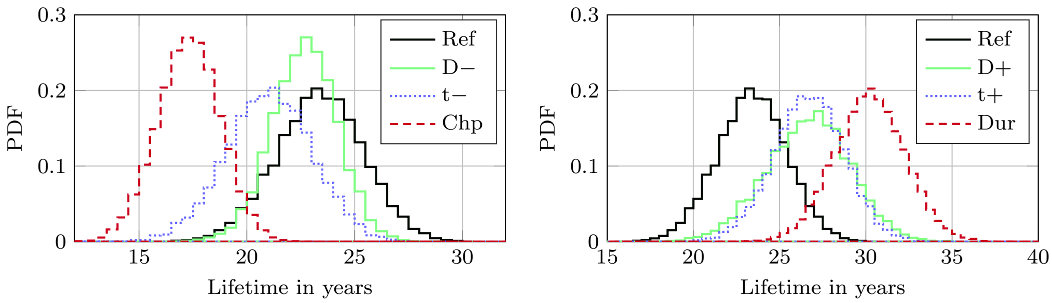

(a) Lifetime PDF for cheaper designs

(b) Lifetime PDF for more durable designs

Figure 5: Lifetime PDF for different substructure designs.

4. Results

4.1. Lifetimes and substructure costs

State-of-the-art design investigations for OWT frequently focus on the structural mass. However, relevant outputs for investors rather concern the cost-efficiency. Consequently, the presented engineering and economic models are combined to focus on the relevant economic results. Nevertheless, as the outputs of the aero-elastic OWT model - substructure lifetimes and CAPEX - are needed for the financial analyses (cf. Fig. 1), first, these intermediate results are presented in brief.
The approximated costs of all seven substructures are summarized in Table 5. The lifetime distributions are shown in Fig. 5 and indicate the effect of design variations on the lifetime. On the one hand, decreased diameters and wall thicknesses result in lower costs. On the other hand, the mean lifetimes of these designs decrease as well. Analogical results are apparent for the durable designs, which have higher costs, but also higher mean lifetimes than the reference design. This trade-off between costs and lifetime leads to opposite effects concerning the profitability and soundness of the OW farm. It has to be further analyzed to assess the overall effect on the cost-efficiency of the substructure designs.
Before analyzing the cost-efficiency, the lifetime distributions are briefly discussed. Figure 5 shows that substructure lifetimes between about 12 and 40 years are possible. If substructure lifetimes are very low for cheap designs, the whole OWT can only be operated for this limited period. However, for durable designs, it is questionable whether the whole OWT can be run for the increased substructure lifetime. Lifetimes of other components (e.g. rotor blades) will limit the overall lifetime in this case. Hence, the positive effect of durable designs is overestimated. Since a lifetime extension of some years for other parts might be possible, while an extension of more than about 10 years is definitely unrealistic, in a second step, the overall lifetime is limited to 20, 25, and 30 years. Exemplary, for a limit of 30 years, the adjusted lifetime PDF are displayed in Fig. 6. Here, the difference to the unlimited lifetime is mainly visible for the durable design. However,

for a limitation of 20 years (not shown), the lifetime distributions of all design are significantly "truncated" and the more durable designs have constant lifetimes of 20 years.

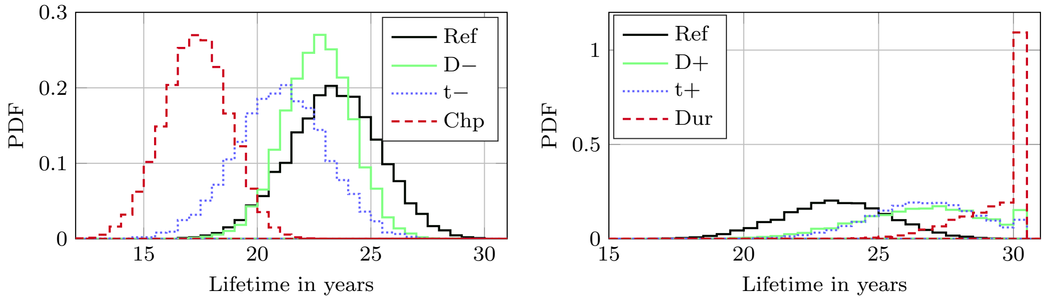

(a) Lifetime PDF for cheaper designs

(b) Lifetime PDF for more durable designs

Figure 6: Lifetime PDF for different substructure designs using a maximum lifetime of 30 years.

4.2. Cost-efficiency

In consideration of the outputs of the aero-elastic OWT model, the economic viability model is applied to the project characteristics of the OW farm given each substructure design separately. Figure 7 shows the results of the optimization model for the reference substructure design. For a sales price of 8.57 ct/kWh, the following applies: $E(APV) = 0$ and $F^{-1}_{DSCR,t}(25\,\%) = 1.2$. The APV PDF mean value is nil (see Fig. 7(a)) and the 25$^{\text{th}}$ percentiles of the DSCR PDF are equal to the DSCR target of 1.2 (see Fig. 7(b)). Hence, the investment criteria of both equity and debt investors are exactly fulfilled, which means that the marginal cost is equal to the estimated sales price. The economic viability model is congruently applied to the other substructure designs. Table 6 shows the calculated marginal cost of all substructure designs and their percentage deviations from the marginal cost of the reference design. To enable an additional design comparison by means of the APV, the resulting APV PDF of the OW farm for each design given the marginal cost of the reference design are shown in Figs. 8 to 10. In addition, the corresponding expected APV and expected unlevered IRR are shown in Table 7. The unlevered IRR is used to compare the results for different substructures, as it is independent of a project's individual leverage which changes for the considered substructure design. As the marginal cost for the reference design is used, the corresponding expected APV is equal to zero and the expected unlevered IRR is equal to the unlevered cost of capital.
The results show that - for the unlimited lifetime ("unltd") - the analyzed OW farm has the lowest marginal cost in consideration of the durable substructure design (Dur), which has the highest cost, but longest expected lifetime. Consequently, following the defined competitiveness criterion, the durable design is the most cost-efficient solution among all substructure designs. Accordingly, the cheapest substructure design (Chp) is least cost-efficient and has the highest marginal cost. Taking all substructure designs into account, the results indicate that the marginal cost decreases with increasing diameters and wall thicknesses. Hence, for the present setup (i.e. turbine, project characteristics, minor design variations, etc.), it holds true that the more durable a substructure design, the more competitive it is compared to the reference design, and vice versa.
As discussed before, an unlimited lifetime is not realistic, as other turbine parts are not considered. If a limitation of the lifetime to 25 or 30 years is introduced ("max25" and "max30"), the APV PDF of the more durable designs feature a negative skewness (see Fig. 9(b)), as they highly dependent on the lifetime PDF that are also skewed due to the "truncation". The positive effects of increased durability decrease, as the total lifetime potential of these substructure designs is not fully used (i.e. the durable design cannot exploit its full lifetime of up to 40 years). This means that the cost-efficiency of the more durable design variations is overestimated for the unlimited case. Nevertheless, although the durable design is overdesigned in the limited cases ("max25" and "max30"), it is still the most cost-efficient one. Hence, for the investigated monopile, it is reasonable to slightly overdesign the substructure to guarantee the design lifetime and even

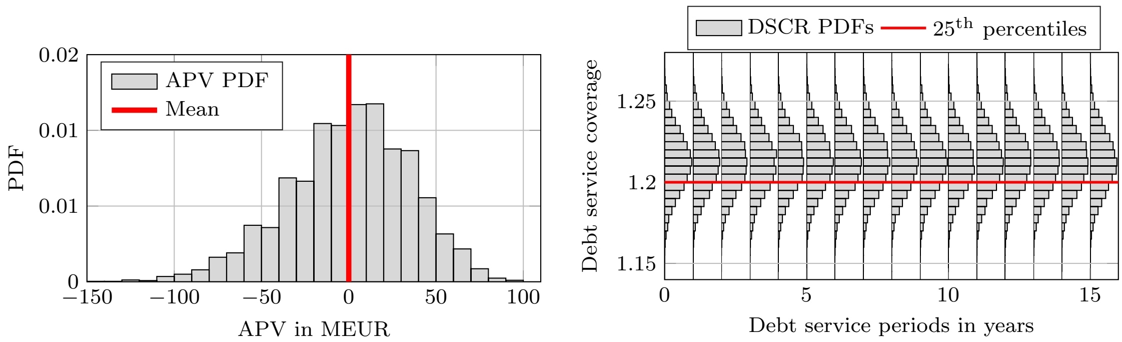

(a) APV PDF for the reference design

(b) DSCR PDF for the reference design

Figure 7: APV and DSCR PDF for the reference substructure design.

a lifetime extension of several years.
If it is assumed that the lifetime of other turbine parts cannot be extended and the overall lifetime is limited to 20 years ("max20"), it becomes clear that a significant overdesign (e.g. the durable design with an expected lifetime of more than 30 years, i.e. the substructure lifetime exceeds the fixed turbine lifetime by 50 % on average) will lead to less cost-efficiency. Table 6 shows that for this case, a cheaper design (D−) is the most cost-efficient solution. This means that in some cases, reduced lifetimes can even be beneficial. Furthermore, variances of the APV PDF decrease significantly given a lifetime limitation of 20 years (cf. Fig. 10(b)), since then, for most designs, the lifetime is constant. Hence, the marginal cost of the substructure designs differs only slightly, except for the cheapest design that features lifetimes below 20 years with a significant probability. From this, it follows that cheap designs with expected lifetimes significantly lower than 20 years should be avoided and that longer lifetimes using more durable designs are promising in most cases.
The results for the expected APV and unlevered IRR shown in Table 7 confirm the findings from the comparison according to the marginal cost. The highest expected APV can be achieved with the most durable substructure design. The cheapest design results in the lowest expected APV. The same holds true for the unlevered IRR. A comparison of Figs. 8(b) and 9(b) makes clear that the advantage of the durable design decreases for more realistically limited maximum lifetimes. Although the lifetime restriction to 30 years only affects more durable designs (cf. Fig. 6), these designs are still most competitive. In contrast, if lifetimes are strictly limited to the design lifetime of 20 years, all designs are affected (cf. Fig. 10), since for all lifetime PDF, a significant part above 20 years is "truncated". Given this lifetime limitation, the more durable designs lead to quite similar results, as they have nearly constant lifetimes of 20 years. Cheaper designs become much more competitive. In this case, the design with a reduced diameter (D−) is the most cost-efficient one, as it has lower substructure costs (cf. Table 5), but the lifetime still reaches the maximum of 20 years with a probability of about 95 % (cf. Fig. 5). The most durable design (Dur) - being the best design for less limited lifetimes - has even slightly lower expected APV and unlevered IRR than the reference case. The reason are higher CAPEX for the substructure, whereas the lifetime cannot be increased due to the limitation to 20 years.

5. Discussion, limitations and outlook

The effects of substructural design variations on the OW farm's economic viability using an interdisciplinary, probabilistic simulation approach that combines engineering and economic models are analyzed. It becomes apparent that even small changes in the designs can lead to significantly different marginal cost for OW farms. Results indicate that the effect of varying lifetimes exceeds the effect of changes in initial costs. This means that for the considered OW farm, more durable designs with higher lifetimes outperform cheaper designs. This implies strong incentives for investors to make rather sustainable investment decisions

Table 6: Marginal cost (in ct/kWh) given each substructure design and different maximum lifetimes (unltd: unlimited, max30: maximum of 30 years, max25: maximum of 25 years, max20: maximum of 20 years). Best designs in bold.

Design	Marginal cost (in ct/kWh)				Deviation from Ref			
	unltd	max30	max25	max20	unltd	max30	max25	max20
Ref	8.57	8.57	8.59	8.99	0.00 %	0.00 %	0.23 %	4.84 %
D+	8.28	8.28	8.44	8.99	−3.44 %	−3.39 %	−1.57 %	4.91 %
D−	8.64	8.64	8.64	**8.97**	0.76 %	0.76 %	0.79 %	**4.68 %**
t+	8.27	8.27	8.43	9.00	−3.50 %	−3.48 %	−1.71 %	4.94 %
t−	8.85	8.85	8.85	9.03	3.25 %	3.25 %	3.26 %	5.40 %
Dur	**8.03**	**8.08**	**8.41**	9.01	**−6.29 %**	**−5.70 %**	**−1.87 %**	5.08 %
Chp	9.50	9.50	9.50	9.51	10.9 %	10.9 %	10.9 %	10.9 %

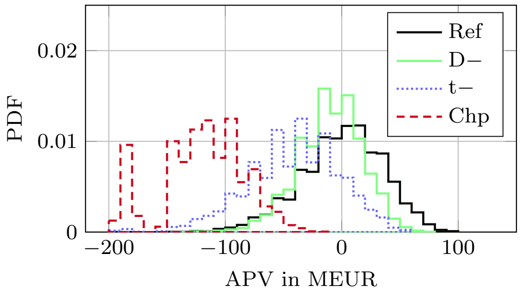

(a) APV PDF for cheaper designs

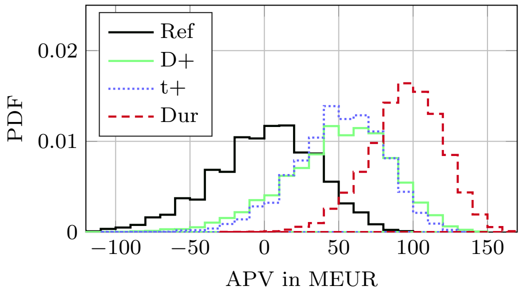

(b) APV PDF for more durable designs

Figure 8: APV PDF for different substructure designs.

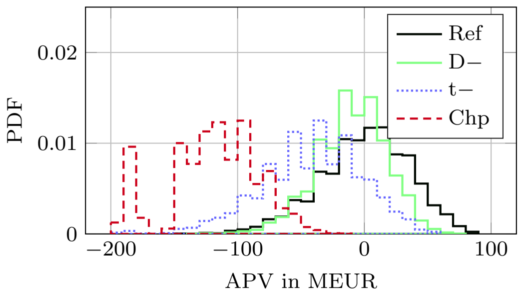

(a) APV PDF for cheaper designs

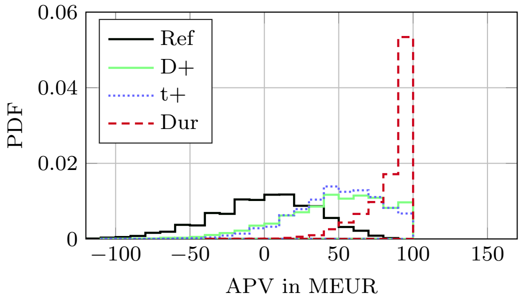

(b) APV PDF for more durable designs

Figure 9: APV PDF for different substructure designs using a maximum lifetime of 30 years.

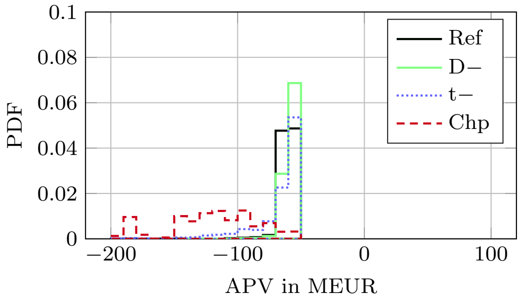

(a) APV PDF for cheaper designs

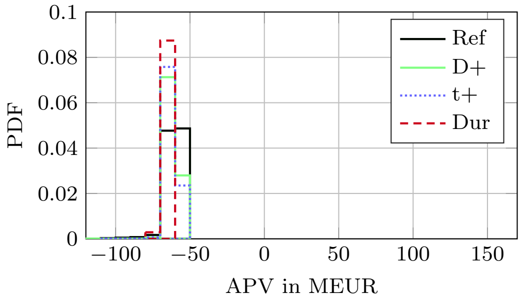

(b) APV PDF for more durable designs

Figure 10: APV PDF for different substructure designs using a maximum lifetime of 20 years.

Table 7: APV and IRR given each substructure design. Best designs in bold.

Design	APV in MEUR				IRR in %			
	unltd	max30	max25	max20	unltd	max30	max25	max20
Ref	0	−0.00	−3.14	−61.0	5.56	5.56	5.52	4.54
D+	49.4	48.6	21.8	−61.9	6.25	6.24	5.91	4.53
D−	−10.1	−10.1	−10.6	**−58.9**	5.42	5.42	5.42	**4.58**
t+	50.4	50.0	23.8	−62.3	6.27	6.27	5.95	4.53
t−	−41.7	−41.7	−41.9	−67.2	4.84	4.84	4.84	4.39
Dur	**95.1**	**85.4**	**26.3**	−64.1	**6.76**	**6.67**	**5.98**	4.50
Chp	−125	−125	−125	−125	2.94	2.94	2.94	2.94

regarding turbine substructures.

The present analyses are limited to a single monopile design (including small design variations). Therefore, a general validity of these results is not given. Especially for other substructure types, the trade-off between lifetime and CAPEX might be differently valued. If the substructure CAPEX are higher, being the case for jackets or floating substructures, the economic advantage of longer lifetimes will be smaller or even diminish. The results of the "max20" case indicate that sometimes it might be even beneficial to reduce lifetimes, if this limits the CAPEX.

For the sake of simplicity, OPEX are considered to be constant for all designs and over time. For a more realistic representation, in future research, the influence of variable OPEX should be investigated as well. Normally, cheaper designs cause higher OPEX. Another limitation of the analyses refers to the constant unlevered cost of capital and the corresponding effect of discounting on the trade-off between lifetime and CAPEX. Higher unlevered cost of capital, as for example, caused by country risk premiums, significantly reduces the impact of cash-flows in later years due to a higher discounting such that the economic effect of lifetime extensions becomes less important, and vice versa.

Regardless the type of effect, the combined engineering and economic analysis clarifies that the lifetime should not be considered as a constant. It should be included as an important variable that has to be optimized relative to the corresponding CAPEX by analyzing the economic effect of their trade-off.

This leads to some open issues that should be addressed by upcoming work: First, so far, only the effect of different designs was analyzed. As noted before, in future optimizations, the OWT lifetime should be regarded as a variable. Hence, such an optimization of the substructure taking into account an optimal lifetime would be beneficial. It might lead to significantly different "optimal" structures compared to optimizations using constant lifetimes. Second, such future optimizations should also consider variable unlevered cost of capital, which depend on the risk inherent to the analyzed substructure design. For example, more durable designs decrease the overall project risk and should thus slightly reduce the unlevered cost of capital due to a lower beta factor (risk measure), and vice versa. This could further increase the cost-efficiency of durable substructure designs. Third, so far, only the design of the substructure was varied. The whole economic viability topic using probabilistic, interdisciplinary analyses can be applied to other turbine parts as well. Hence, upcoming work should also address other components (e.g. blades). The inclusion of other components will probably lead to even more pronounced differences in the marginal cost.

Appendix A

The purpose of this derivation is to show the derivative of the expected APV with respect to the sales price per unit of generated electricity (cf. Eq. 18):

$$\frac{dE(APV)}{dp} = (1-\tau) \cdot \sum_{t=0}^{T} \frac{E(Y_t)}{(1+r_e)^t} + \tau \cdot (1-\tau) \cdot \sum_{t=0}^{T_{Debt}} \frac{\frac{F_{Y,t}^{-1}(\alpha)}{\beta}}{(1+r_d)^t} \cdot (1-(1+r_d)^{-t}).$$

The starting point is the adjusted present value in Eq. 14. The APV can be split in two addends, the unlevered APV ($uAPV_t$) and the discounted tax shield (DTS_t):

$$
\begin{aligned}
APV &= \sum_{t=0}^{T} \frac{FCF_t}{(1+r_e)^t} + \frac{\tau \cdot INT_t}{(1+r_d)^t} \\
&= \sum_{t=0}^{T} uAPV_t + DTS_t.
\end{aligned}
$$

$$
\frac{dE(APV)}{dp} = \frac{d}{dp} E\left[\sum_{t=0}^{T} uAPV_t\right] + \frac{d}{dp} E\left[\sum_{t=0}^{T_{Debt}} DTS_t\right].
$$

Using Table 3, the first addend of the APV equation - the unlevered APV - can be rearranged as follows, where we denote depreciation as DEP, decommissioning expenses as $DECEX$, its provisions as PDC, and the taxes on EBIT as TAX_t:

$$
\begin{aligned}
\frac{d}{dp} E\left[\sum_{t=0}^{T} uAPV_t\right] &= \frac{d}{dp} E\left[\sum_{t=0}^{T} \frac{FCF_t}{(1+r_e)^t}\right] \\
&= \frac{d}{dp} E\left[\sum_{t=0}^{T} \frac{EBIT_t - TAX_t - CAPEX_t - DECEX_t + DEP_t + PDC_t}{(1+r_e)^t}\right].
\end{aligned}
$$

It is assumed that $CAPEX_t$, $DECEX_t$, DEP_t, and PDC_t are independent of p and constant in our case. Therefore, we can simplify as follows:

$$
\begin{aligned}
\frac{d}{dp} E\left[\sum_{t=0}^{T} uAPV_t\right] &= \frac{d}{dp} E\left[\sum_{t=0}^{T} \frac{EBIT_t - TAX_t}{(1+r_e)^t}\right] \\
&= \frac{d}{dp} E\left[\sum_{t=0}^{T} \frac{EBIT_t - \tau \cdot EBIT_t}{(1+r_e)^t}\right] \\
&= \frac{d}{dp} E\left[\sum_{t=0}^{T} \frac{EBIT_t \cdot (1-\tau)}{(1+r_e)^t}\right] \\
&= \frac{d}{dp} E\left[\sum_{t=0}^{T} \frac{(R_t - (OPEX_t + DEP_t + PDC_t)) \cdot (1-\tau)}{(1+r_e)^t}\right].
\end{aligned}
$$

DEP_t, and PDC_t are still independent of p and constant. The same holds true for $OPEX_t$. However, it is conceivable that specific contractual arrangements feature dependency on the revenues and thus on the price p. An example could be the land lease. As we assume turbine dependent $OPEX_t$, they are independent of p and constant in our case. It follows:

$$
\begin{aligned}
\frac{d}{dp} E\left[\sum_{t=0}^{T} uAPV_t\right] &= \frac{d}{dp} E\left[\sum_{t=0}^{T} \frac{R_t \cdot (1-\tau)}{(1+r_e)^t}\right] \\
&= \frac{d}{dp} E\left[\sum_{t=0}^{T} \frac{Y_t \cdot p \cdot (1-\tau)}{(1+r_e)^t}\right] \\
&= (1-\tau) \cdot \sum_{t=0}^{T} \frac{E(Y_t)}{(1+r_e)^t}.
\end{aligned}
$$

For the second addend - the tax shield (TS_t), Eqs. 9 to 13 and Table 3 are used for the following rearrangements:

$$\begin{aligned}
\frac{d}{dp}E\left[\sum_{t=0}^{T_{Debt}} DTS_t\right] &= \frac{d}{dp}E\left[\sum_{t=0}^{T_{Debt}} \frac{TS_t}{(1+r_d)^t}\right] \\
&= \frac{d}{dp}E\left[\sum_{t=0}^{T_{Debt}} \frac{\tau \cdot INT_t}{(1+r_d)^t}\right] \\
&= \frac{d}{dp}E\left[\sum_{t=0}^{T_{Debt}} \frac{\tau \cdot (DSC_t - P_t)}{(1+r_d)^t}\right] \\
&= \frac{d}{dp}E\left[\sum_{t=0}^{T_{Debt}} \frac{\tau \cdot \left(DSC_t - \frac{DSC_t}{(1+r_d)^t}\right)}{(1+r_d)^t}\right] \\
&= \frac{d}{dp}E\left[\sum_{t=0}^{T_{Debt}} \frac{\tau \cdot DSC_t}{(1+r_d)^t} \cdot \left(1 - (1+r_d)^{-t}\right)\right] \\
&= \frac{d}{dp}E\left[\sum_{t=0}^{T_{Debt}} \frac{\tau \cdot \frac{F^{-1}_{FCF,t}(\alpha)}{\beta}}{(1+r_d)^t} \cdot \left(1 - (1+r_d)^{-t}\right)\right].
\end{aligned}$$

As before, FCF can be expressed as:

$$FCF = (Y_t \cdot p - OPEX_t + DEP_t + PDC_t)(1-\tau) - CAPEX_t - DECEX_t + DEP_t + PDC_t$$

and $OPEX_t$, $CAPEX_t$, $DECEX_t$, DEP_t, and PDC_t are independent of p and in our case constant. Therefore, it holds:

$$F^{-1}_{FCF,t}(\alpha) = F^{-1}_{Y,t}(\alpha) \cdot p \cdot (1-\tau) + c$$

where, $c = -(OPEX_t + DEP_t + PDC_t)(1-\tau) - CAPEX_t - DECEX_t + DEP_t + PDC_t$. We can further rearrange the second addend:

$$\frac{d}{dp}E\left[\sum_{t=0}^{T_{Debt}} DTS_t\right] = \frac{d}{dp}E\left[\sum_{t=0}^{T_{Debt}} \frac{\tau \cdot \frac{F^{-1}_{Y,t}(\alpha)\cdot p\cdot(1-\tau)+c}{\beta}}{(1+r_d)^t} \cdot \left(1 - (1+r_d)^{-t}\right)\right].$$

Since the previous term does not contain any random variable, the expected value of the term is the term itself, it follows:

$$\frac{d}{dp}E\left[\sum_{t=0}^{T_{Debt}} DTS_t\right] = \tau \cdot (1-\tau) \cdot \sum_{t=0}^{T_{Debt}} \frac{\frac{F^{-1}_{Y,t}(\alpha)}{\beta}}{(1+r_d)^t} \cdot (1 - (1+r_d)^{-t}).$$

Finally, the full expression in Eq. 18 is:

$$\begin{aligned}
\frac{dE(APV)}{dp} &= \frac{d}{dp}E\left[\sum_{t=0}^{T} uAPV_t\right] + \frac{d}{dp}E\left[\sum_{t=0}^{T_{Debt}} DTS_t\right] \\
&= (1-\tau) \cdot \sum_{t=0}^{T} \frac{E(Y_t)}{(1+r_e)^t} + \tau \cdot (1-\tau) \cdot \sum_{t=0}^{T_{Debt}} \frac{\frac{F^{-1}_{Y,t}(\alpha)}{\beta}}{(1+r_d)^t} \cdot (1 - (1+r_d)^{-t}).
\end{aligned}$$

Acknowledgements

We gratefully acknowledge the financial support of the European Commission (research project IRPWind, funded from the European Union's Seventh Framework Programme for research, technological development and demonstration under grant agreement number 609795) that enabled this work.
This work was supported by the compute cluster, which is funded by Leibniz Universität Hannover, the Lower Saxony Ministry of Science and Culture (MWK) and the German Research Association (DFG).

References

[1] J. K. Kaldellis, D. Apostolou, Life cycle energy and carbon footprint of offshore wind energy. comparison with onshore counterpart, Renewable Energy 108 (2017) 72–84.
[2] C. Brown, R. Poudineh, B. Foley, Achieving a cost-competitive offshore wind power industry: What is the most effective policy framework?, Tech. rep., Oxford Institute for Energy Studies (2015).
[3] Energy Information Administration, Levelized cost and levelized avoided cost of new generation resources in the annual energy outlook 2017, Tech. rep., U.S. Energy Information Administration (EIA) (2017).
[4] A. Mbistrova, A. Nghiem, The value of hedging - new approaches to managing wind energy resource risk, Tech. rep., Wind Europe (2017).
[5] Prognos AG and Fichtner, Kostensenkungspotenziale der Offshore-Windenergie in Deutschland, Tech. rep., Stiftung Offshore-Windenergie (2013).
[6] Y. S. Lee, B. L. Choi, J. H. Lee, S. Y. Kim, S. Han, Reliability-based design optimization of monopile transition piece for offshore wind turbine system, Renewable Energy 71 (2014) 729–741.
[7] D. Kallehave, B. W. Byrne, C. L. Thilsted, K. K. Mikkelsen, Optimization of monopiles for offshore wind turbines, Philosophical Transactions of the Royal Society 373 (2015) 20140100.
[8] J. Häfele, R. Rolfes, Approaching the ideal design of jacket substructures for offshore wind turbines with a particle swarm optimization algorithm, in: ISOPE Conference, Rhodes, Greece, 2016, pp. 156–163.
[9] J. Oest, R. Sørensen, L. C. T. Overgaard, E. Lund, Structural optimization with fatigue and ultimate limit constraints of jacket structures for large offshore wind turbines, Structural and Multidisciplinary Optimization 55 (3) (2017) 779–793.
[10] M. Muskulus, S. Schafhirt, Design optimization of wind turbine support structures - a review, Journal Ocean Wind Energy 1 (1) (2014) 12–22.
[11] M. Maness, B. Maples, A. Smith, Nrel offshore balance-of-system model, Tech. rep., National Renewable Energy Laboratory (2017).
[12] J. Farkas, K. Jármai, Optimum design of steel structures, Springer, Heidelberg, 2013.
[13] L. Ziegler, M. Rhomberg, M. Muskulus, Optimization of monopiles with genetic algorithms: How does steel mass increase if offshore wind monopiles are designed for a longer service life?, Journal of Physics: Conference Series 1104 (2018) 012014.
[14] O. Salo, S. Syri, What economic support is needed for arctic offshore wind power?, Renewable and Sustainable Energy Reviews 31 (2014) 343 – 352.
[15] N. Ederer, The right size matters: Investigating the offshore wind turbine market equilibrium, Energy 68 (2014) 910 – 921.
[16] D. E. Gernaat, D. P. V. Vuuren, J. V. Vliet, P. Sullivan, D. J. Arent, Global long-term cost dynamics of offshore wind electricity generation, Energy 76 (2014) 663 – 672.
[17] H. L. Raadal, B. I. Vold, A. Myhr, T. A. Nygaard, GHG emissions and energy performance of offshore wind power, Renewable Energy 66 (2014) 314 – 324.
[18] S. Afanasyeva, J. Saari, M. Kalkofen, J. Partanen, O. Pyrhönen, Technical, economic and uncertainty modelling of a wind farm project, Energy Conversion and Management 107 (2016) 22 – 33, special Issue on Efficiency, Cost, Optimisation, Simulation and Environmental Impact of Energy Systems (ECOS)-2014.
[19] M. Batchelor, Feasibility of offshore wind in australia, Ph.D. thesis, Murdoch University (2012).
[20] T. Rubert, D. McMillan, P. Niewczas, A decision support tool to assist with lifetime extension of wind turbines, Renewable Energy 120 (2018) 423 – 433.
[21] Wind turbines – Part 3: Design requirements for offshore wind turbines. IEC-61400-3 (2009).
[22] J. Jonkman, The new modularization framework for the FAST wind turbine CAE tool, in: 51st AIAA Aerospace Sciences Meeting, including the New Horizons Forum and Aerospace Exposition, no. NREL/CP-5000-57228, Dallas, United States, 2013.
[23] J. Jonkman, S. Butterfield, W. Musial, G. Scott, Definition of a 5-MW reference wind turbine for offshore system development, Tech. rep., National Renewable Energy Lab (2009).
[24] C. Bak, F. Zahle, R. Bitsche, T. Kim, A. Yde, L. C. Henriksen, M. H. Hansen, J. P. A. A. Blasques, M. Gaunaa, A. Natarajan, The dtu 10-mw reference wind turbine, in: Danish Wind Power Research, 2013.
[25] J. M. Jonkman, W. Musial, Offshore code comparison collaboration (OC3) for IEA task 23 offshore wind technology and deployment, Technical Report NREL/TP-5000-48191, National Renewable Energy Laboratory, Golden, CO (2010).
[26] C. Hübler, C. G. Gebhardt, R. Rolfes, Development of a comprehensive database of scattering environmental conditions and simulation constraints for offshore wind turbines, Wind Energy Science 2 (2017) 491–505.
[27] J. Jonkman, L. Kilcher, Turbsim user's guide: Version 1.06.00, Tech. rep., National Renewable Energy Laboratory (2012).

[28] C. Hübler, C. G. Gebhardt, R. Rolfes, Methodologies for fatigue assessment of offshore wind turbines considering scattering environmental conditions and the uncertainty due to finite sampling, Wind Energy 21 (11) (2018) 1092–1105.
[29] D. Zwick, M. Muskulus, The simulation error caused by input loading variability in offshore wind turbine structural analysis, Wind Energy 18 (8) (2015) 1421–1432.
[30] Eurocode 3: Design of steel structures - part 1-9: Fatigue. EN 1993-1-9 (2010).
[31] C. Bjerkseter, A. Ågotnes, Levelised costs of energy for offshore floating wind turbine concepts, Master's thesis, Norwegian University of Life Science (2013).
[32] W. de Vries, N. Vemula, P. Passon, T. Fischer, D. Kaufer, D. Matha, B. Schmidt, F. Vorpahl, Final report WP 4.2: Support structure concepts for deep water sites: Deliverable d4.2.8, Tech. rep., Delft University of Technology (2011).
[33] E. de Vries, Foundations built on corrosion protection, Windpower offshore, 30 September 2014.
[34] J.-H. Piel, J. F. Hamann, A. Koukal, M. H. Breitner, Promoting the system integration of renewable energies: Toward a decision support system for incentivizing spatially diversified deployment, Journal of Management Information Systems 34 (4) (2017) 994–1022.
[35] B. Reimers, M. Kaltschmitt, Kostenentwicklung der Offshore-Windstromerzeugung - Analyse mithilfe der Erfahrungskurventheorie, Zeitschrift für Energiewirtschaft 38 (4) (2014) 217–234.
[36] Bloomberg New Energy Finance, New energy outlook 2016, Tech. rep. (2017).
[37] Global Wind Energy Council, Global wind report 2016 – annual market update, Tech. rep. (2017).
[38] B. Steffen, The importance of project finance for renewable energy projects, Energy Economics 69 (2018) 280–294.
[39] L. Lang, E. Ofek, R. Stulz, Leverage, investment, and firm growth, Journal of financial Economics 40 (1) (1996) 3–29.
[40] C. McInerney, D. W. Bunn, Optimal over installation of wind generation facilities, Energy Economics 61 (2017) 87–96.
[41] F. S. Mishkin, The economics of money, banking, and financial markets, 11th Edition, Pearson education, 2016.
[42] S. C. Myers, Interactions of corporate financing and investment decisions—implications for capital budgeting, The Journal of finance 29 (1) (1974) 1–25.
[43] J. Sabal, Wacc or apv?, Journal of Business Valuation and Economic Loss Analysis 2 (2) (2007) 1–17.
[44] A. Koukal, M. H. Breitner, Offshore wind energy in emerging countries: A decision support system for the assessment of projects, in: Proceedings of the 47th HICSS, Hawaii, United States, 2014, pp. 865–874.
[45] L. Werner, B. Scholtens, Firm type, feed-in tariff, and wind energy investment in germany: An investigation of decision making factors of energy producers regarding investing in wind energy capacity, Journal of Industrial Ecology 21 (2) (2017) 402–411.